Diffusion MRI and Contrast-Enhanced Monitoring of Prostate Microwave Focal Thermal Therapy: an In-Vivo Canine Study

H-L. M. Cheng[1,2], M. A. Haider[3], M. J. Dill-Macky[4], J. M. Sweet[5], J. Trachtenberg[6], and M. R. Gertner[7,8]

[1]Research Institute & Diagnostic Imaging, The Hospital for Sick Children, Toronto, Ontario, Canada, [2]Medical Biophysics, University of Toronto, Toronto, Ontario, Canada, [3]Medical Imaging, University Health Network and Mount Sinai Hospital, [4]Pathology & Laboratory Medicine, University Health Network, [5]Pathology & Laboratory Medicine, University Health Network, University of Toronto, [6]Surgery, University Health Network, [7]Biophysics & Bioimaging, University Health Network, [8]Physics, Ryerson University

INTRODUCTION

Non-invasive image monitoring of thermal ablation is valuable for treatment guidance and immediate assessment. Contrast-enhanced (CE) methods have been particularly useful, where the non-enhancing area is known to depict the lesion [1-3]. Potentially better and more repeatable than the contrast approach is diffusion MRI, which in a few studies has shown a reduced apparent diffusion coefficient (ADC) in the necrotic area of both frozen [4] and heated tissues [5]. However, the ADC characteristics have not been studied for microwave heating of the prostate and have not been compared to CE findings. In this study, we evaluate three approaches (diffusion MRI, CE-MRI, and CE ultrasound (CEUS)) in interstitial microwave heating of the normal prostate and show that the ADC may provide the most accurate and distinct delineation of lesion boundaries.

METHODS

Seven beagle dogs (8.5-14 kg) underwent microwave heating of the prostate, followed by CEUS, MRI, and sacrifice approximately 2 hours post-heating. Microwave energy (915 MHz) was delivered from a BSD-500 Precision Hyperthermia System through two antennas (model MA250 helical coil tip, BSD Medical Systems Inc.) inserted into the mid-left and right lobes. CEUS was performed with Definity® microbubbles (1.1-3.3 μm) using both bolus injections and drip infusions. MRI was performed on a 1.5-T scanner (Signa EXCITE TwinSpeed, GE) using an 8-channel head coil. Diffusion MRI was acquired using a 2D SE-EPI [TR/TE=4000/64 ms, b-value=600 s/mm^2, NEX=8, 128×238 matrix, SL=4 mm]. Contrast agent (Magnevist, Bayer HealthCare) was given as a bolus (0.1 mmol/kg) and monitored over 3.5 minutes using a T1-weighted 3D fast spoiled gradient echo [TR/TE= 6.15/2.0 ms, FA=25°, NEX=0.5, 256×128×12 matrix, SL=4 mm, time resolution=4.7 s]. Animals were immediately sacrificed after MRI and the prostate removed for photographs and whole-mount histology (H&E).

The MRI datasets were then analyzed pixel-by-pixel for the ADC and initial area under the uptake curve (IAUC) [6]. MRI and CEUS images were then segmented for comparison to histology, using a preset threshold for ADC and IAUC maps (halfway between minimum and that in normal prostate) and manual segmentation for CEUS.

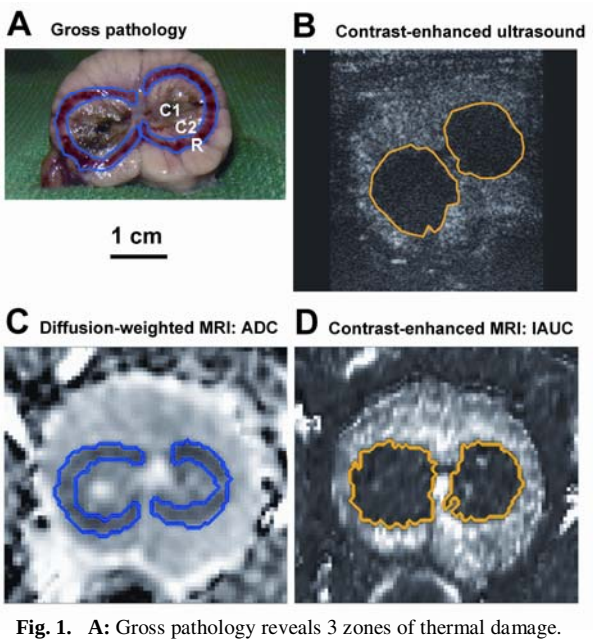

Fig. 1. **A:** Gross pathology reveals 3 zones of thermal damage. **B-D:** Ultrasound and MRI (segmented regions in color).

RESULTS

Fig.1A shows three zones of the thermal lesion: a central brown region (C1) of intact but coagulated tissue, another coagulation region (C2) with disrupted cell membranes and interstitial edema, and a red ring (R) characterized by hyperemia with vascular dilatation and hemorrhage. Contrast-enhanced imaging revealed a non-enhancing core (Fig.1B,D); its measured area on MRI and CEUS were correlated (r =0.997, P <0.001). The IAUC in the core (0.96±0.05) was significantly lower than in unheated prostate (1.96±0.44, P<10^{-5}). In 8 of the 11 lesions, an enhancing rim (IAUC=2.78±0.54, P<0.01) with a diffuse outer border was also present. Diffusion imaging (Fig.1C) always revealed a well delineated ring of reduced ADC relative to unheated prostate (1.03±0.12 vs. 1.60±0.12 × 10^{-3} mm^2/s, P<10^{-6}).

Segmented regions on diffusion and CE images shown in Fig.1 occupy different spatial locations and reveal distinct thermal changes. The ADC ring corresponds to the red ring (R), with high correlations obtained for the inner (r=0.993, P<0.001; slope=1.05) and outer borders (r=0.996, P<0.001; slope=0.994). The lowered ADC is consistent with restricted water diffusion in a region of vascular congestion and interstitial hemorrhage. In contrast, the borders of the non-enhancing core (low IAUC) did not correlate with any histological zone but were located within Zone R (i.e. ADC ring (Fig.2)). This sharp decrease in contrast enhancement signifies blood flow cessation and is consistent with the transition within the red ring from hyperemia (ring periphery) to thrombosis and hemorrhage (central part of ring).

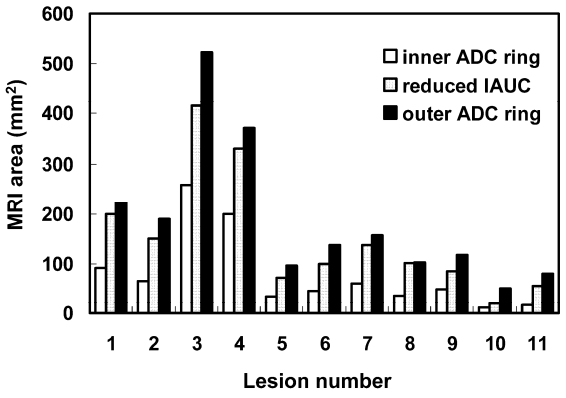

Fig. 2. The area of reduced IAUC on contrast-enhanced MRI is smaller than the area enclosed by the outer ADC ring.

CONCLUSIONS

Diffusion MRI of a microwave-induced thermal lesion in the prostate reveals lowered ADC in a well-defined ring, not throughout the lesion as seen in other applications. This ADC ring is larger than the non-enhancing core on conventional CE MRI or US images, and is shown in this study to correspond to the red ring of thermal damage known to represent the eventual full extent of necrosis in the days following therapy [7]. An enhancing rim on CE imaging may provide similar information to the ADC ring, but it appears only in some lesions and its borders are too diffuse compared to the ADC ring for accurate determination. Diffusion MRI may be more accurate than CE imaging to predict tissue necrosis.

REFERENCES: [1] Cheng HL, et al. JMRI 2003; 18:585. [2] Hazle JD, et al. JMRI 2002; 15:409. [3] Liu JB, et al. J Urol 2006; 176:1654. [4] Butts K, et al. JMRI 2003; 17:131. [5] Jacobs MA, et al. Radiology 2005; 236:196. [6] Evelhoch JL. JMRI 1999; 10:254. [7] Thomsen S. Proceedings of SPIE. 1999; 3594:82.